

Deflection Analysis of Electrostatic Micro-actuators Using the Differential Quadrature Method

Ming-Hung Hsu

*Department of Electrical Engineering, National Penghu University,
Penghu, Taiwan 880, R.O.C.*

Abstract

The nonlinear pull-in behaviors of various electrostatic micro-actuators were simulated. The differential quadrature method (DQM) was applied to overcome the difficulty in solving the nonlinear equation of motion. Various types of micro-actuators, such as the cantilever beam actuator and the fixed-fixed beam actuator were derived and simulated to examine the feasibility of applying the DQM to the nonlinear deflection in solving the micro-actuator problem. The calculated results agreed very closely with those in the literature. This study presents a nonlinear deflection analysis of electrostatic curved electrode actuators using the DQM. The characteristics of various combinations of shaped cantilevers and curved electrodes are also considered to optimize the design. The determination of the static deflections of the uniform actuator and the non-uniform actuator using the DQM is efficient. The deflections of non-uniform actuators with various voltages are obtained. Numerical results are compared with experimental results to derive the efficient and systematic procedure for solving nonlinear differential equations.

Key Words: Microelectromechanical System, Pull-in, Electrostatic, DQM

1. Introduction

As the use of fast computers and the range of available numerical methods, including the Rayleigh-Ritz method, the Galerkin method, the finite element method and the boundary element method, the solutions to numerous complex beam-shape problems have been efficiently obtained. However, an alternative technique with improved computational efficiency and numerical accuracy is sought. Bellman et al. introduced the differential quadrature method (DQM) [1,2]. The DQM has been widely used to solve a variety of problems in different fields of science and engineering. The DQM has been shown to be a powerful candidate for in solving initial and boundary value problems and has thus become an alternative to other methods. DQM is applied extensively in structural mechanics. Bert et al. [3–8] analyzed the static and free vibration of beams and rectan-

gular plates using the DQM. Jang et al. [9] proposed the δ method. The boundary points are selected at a small distance from each other. The δ technique can be applied to the double boundary conditions of plate and beam problems. The δ must not be enlarged to increase the accuracy of the solution. The solutions oscillate when the δ is too small. Wang and Bert [10] consider the boundary conditions in evaluating the weighting coefficients. Malik and Bert [11] solved the free vibration of the plates and demonstrated that the boundary conditions can be incorporated into the weighting coefficients. In this formulation, the multiple boundary conditions are directly applied to the weighting coefficients so, unlike by the δ -interval method, no nearby point needs to be selected. Restated, the accuracy of the calculated results is independent of the value of the δ -interval. The weighting coefficients can be obtained by multiplying of the inverse matrix. Quan and Chang [12,13] derived the weighting coefficients in more explicitly. The explicit formulae can be applied conveniently.

*Corresponding author. E-mail: hsu@npu.edu.tw

Sherbourne and Pandey [14] analyzed buckling behavior using the DQM. Feng and Bert [15] analyzed vibration problem of a geometrically nonlinear beam using the DQM. Du et al. [16] analyzed structural problems using the DQM. Wang et al. [17] analyzed vibration problem of circular annular plates with non-uniform thickness using the DQM. Liew et al. [18] analyzed mindlin plates on winkler foundations problem using the DQM. Liew et al. [19] analyzed thick symmetric cross-ply laminates with first-order shear flexibility problem using the DQM. Du et al. [20] analyzed buckling problem using the DQM. Kang et al. [21] analyzed static problem of a curved shaft subjected to end torques using the DQM. Mirfakhraei and Redekop [22] analyzed buckling problem of circular cylindrical shells using the DQM. Tomasiello [23] analyzed initial-boundary-value problems using the DQM. Moradi and Taheri [24] presented buckling analysis of general laminated composite beams using the DQM. Hsu [25] analyzed the nonlinear dynamic behavior of an edge-cracked beam on elastic foundation with axial using the DQM. Han and Liew [26] analyzed axisymmetric free vibration problem of thick annular plates using the DQM. De Rosa and Franciosi [27] solved dynamic problem of circular arches using the DQM. Sun and Zhu [28] analyzed incompressible viscous flow problem using the DQM. Tanaka and Chen [29] analyzed transient elastodynamic problems using the DQM. It is not applicable to solve problem have discontinuity in geometry using the DQM. Striz et al. [30] undertook static analysis of structures using the differential quadrature element method. It is applicable to solve problem have discontinuity in geometry using the differential quadrature element method. Wang and Gu [31] analyzed static problem of frame structures using the differential quadrature element method. Gu and Wang [32] analyzed free vibration problem of circular plates with stepped thickness over a concentric region using the differential quadrature element method. Chen [33] presented the warping torsion bar model using the differential quadrature element method. Chen et al. [34] analyzed high-accuracy plane stress and plate elements problem using the differential quadrature element method.

The DQM has been demonstrated to be a strong candidate for solving initial and boundary value problems

and thus has become an alternative to the other methods. The efficiency and the accuracy of Rayleigh-Ritz method are depending on the number and accuracy of the selected comparison functions. However, the DQM does not raise such a difficulty, in terms of selecting the appropriated comparison functions.

Beam-type electrostatic actuators fabricated from silicon have been widely applied in microelectromechanical systems. Petersen [35] first described the nonlinear pull-in behavior of an electrostatic micro-actuator. Osterberg et al. [36] proposed different numerical models to analyze electrostatically deformed diaphragms. The results revealed that the electrostatic deformation calculated using the one-dimensional model is close to that obtained using a three-dimensional model. Various models, the lumped parallel-plate spring model, the one-dimensional numerical model and the finite element model that incorporates a three-dimensional simulation were proposed to calculate the pull-in behaviors of various fixed-fixed DMD structures and pressure sensors [36]. Gilbert et al. [37] analyzed the three dimensional coupled electro-mechanics of MEMS using a CoSolve-EM simulation algorithm. Elwenspoek et al. [38] studied the dynamic behavior of active joints for various electrostatic actuator designs. Legtenberg et al. [39,40] proposed the use of a curved electrode to improve the pull-in performance. These studies applied the Rayleigh-Ritz method to calculate the static deflections of various electrostatic actuators. The cantilever beam model was presented to elucidate the characteristics of actuators with large displacements. Hirai et al. [41–43] considered the deflection characteristics of electrostatic actuators with shaped modified electrodes and cantilevers. Wang [44] applied feedback control to suppressing the vibration of an actuator beam in an electrostatic actuator. Shi et al. [45] presented a combination of an exterior boundary element method for electrostatics and a finite element method for elasticity to evaluate the effect of coupling between the electrostatic force and the elastic deformation. Osterberg and Senturia [46] adopted the sharp instability phenomena of electrostatic pull-in behaviors for cantilever beam and fixed-fixed beam actuators to elicit the material characteristics of MEMS. Gretillat et al. [47] employed the three-dimensional MEMCAD and FEM programs to simulate the dynamics of a nonlinear actuator, considering the effect of squeeze-film damping. Hung and

Senturia [48] developed leveraged bending and strain-stiffening methods to increase the limiting travel distance before pull-in of electrostatic actuators. Chan et al. [49] measured the pull-in voltage and capacitance-voltage and performed 2-D simulations that included the electrical effects of fringing fields and finite beam thickness, to determine the material properties of electrostatic micro-actuators. Electrostatic micro-actuators can undergo large deformations at large applied voltages, so Li and Aluru [50] developed a mixed-regime approach for combining linear and nonlinear theories. Chyuan et al. [51–53] established the validity and accuracy of the dual boundary element method and to study the effect of gap size variation for the levitation of MEMS combdrive.

In this work, the DQM is employed to analyze the nonlinear pull-in behaviors of different types micro-actuators with various load and electrode shapes. This work studies the effect of the shape of the electrode on the static deflection of an electrostatic actuator. The change in the shape of an electrode of an electrostatic actuator is an effective method of varying the distribution of electrostatic forces in the micro-electrostatic actuator. Recently, numerous new actuator designs have been proposed to reduce improving the pull-in weakness. The DQM was employed to formulate the electrostatic field problems in matrix form. The Chebyshev-Gauss-Lobatto point distribution on each actuator is utilized. The integrity and computational accuracy of the DQM in solving this problem will be evaluated through a range of case studies.

2. The Differential Quadrature Method

The core of the DQM is that the derivative of a function at a sample point can be approximated as a weighted linear summation of the value of the function at all of the sample points in the domain. Using this approximation, the differential equation is reduced to a set of algebraic equations. The number of equations depends on the selected number of sample points. Like that of any polynomial approach, the accuracy of the solution using this method is improved by increasing the number of sample points. Possible oscillations in the numerical results associated with higher-order polynomials can be avoided by applying numerical interpolation methods.

For a function $f(z)$, the DQM approximation to the m^{th} order derivative at the i^{th} sampling point is given by

$$\frac{d^m}{dz^m} \begin{Bmatrix} f(z_1) \\ f(z_2) \\ \vdots \\ f(z_N) \end{Bmatrix} \cong [D_{ij}^{(m)}] \begin{Bmatrix} f(z_1) \\ f(z_2) \\ \vdots \\ f(z_N) \end{Bmatrix} \quad (1)$$

for $i, j = 1, 2, \dots, N$

where $f(z_i)$ is the value of the function at the sample point z_i , and $D_{ij}^{(m)}$ are the weighting coefficients of the m^{th} -order differentiation attached to these functional values.

Quan et al. [12,13] introduced a Lagrangian interpolation polynomial to overcome the numerical ill-conditions in determining the weighting coefficients $D_{ij}^{(m)}$:

$$f(z) = \sum_{i=1}^N \frac{M(z)}{(z-z_i)M_1(z_i)} f(z_i) \quad (2)$$

where

$$M(z) = \prod_{j=1}^N (z - z_j),$$

$$M_1(z_i) = \prod_{j=1, j \neq i}^N (z_i - z_j) \quad \text{for } i = 1, 2, \dots, N$$

Substituting Eq. (2) into Eq. (1) yields,

$$D_{ij}^{(1)} = \frac{M_1(z_i)}{(z_j - z_i)M_1(z_j)} \quad (3)$$

for $i, j = 1, 2, \dots, N$ and $i \neq j$

and

$$D_{ii}^{(1)} = - \sum_{j=1, j \neq i}^N D_{ij}^{(1)} \quad \text{for } i = 1, 2, \dots, N \quad (4)$$

After the sample points have been selected, the coefficients of the weighting matrix can be obtained from Eqs. (3) and (4). The number of the test functions must exceed the highest order of the derivative in the governing equations; that is $N > m$.

Higher-order derivatives of weighting coefficients can also be obtained by matrix multiplication: [10,11]

$$D_{ij}^{(2)} = \sum_{k=1}^N D_{ik}^{(1)} D_{kj}^{(1)} \quad \text{for } i, j = 1, 2, \dots, N \quad (5)$$

$$D_{ij}^{(3)} = \sum_{k=1}^N D_{ik}^{(1)} D_{kj}^{(2)} \quad \text{for } i, j = 1, 2, \dots, N \quad (6)$$

$$D_{ij}^{(4)} = \sum_{k=1}^N D_{ik}^{(1)} D_{kj}^{(3)} \quad \text{for } i, j = 1, 2, \dots, N \quad (7)$$

The most convenient approach solving a beam structure problem is to uniformly space out the sample points. The selection of sample points is important in the accuracy of the solution of the DQM. Inaccurate results were obtained using this uniform distribution. A non-uniform sample point distribution, such as Chebyshev-Gauss-Lobatto distribution [5,9], improves the accuracy of the calculation. The unequally spaced, Chebyshev-Gauss-Lobatto-distributed sample points on each beam in this computation satisfy

$$z_i = \frac{L}{2} \left[1 - \cos \frac{(i-1)\pi}{N-1} \right] \quad \text{for } i, j = 1, 2, \dots, N \quad (8)$$

The Chebyshev-Gauss-Lobatto distribution of points on each beam is employed. The integrity and computational efficiency of the DQM in solving this problem will be demonstrated using through a set of case studies. As the availability of various numerical methods, such as the finite difference method, the finite element method and the boundary element method, the static and dynamic solutions for numerous complicated structures have become obtainable. However, an alternative efficient technique is still sought.

3. Static Deflections of the Electrostatic Actuators

Figure 1 depicts the geometry of a tapered electrostatic actuator; t_0 specifies the thickness at the root of the actuator and t_1 represents the thickness at the tip. L is the length of the actuator. P and $q(z)$ are the loads. Load P acts on the tip of the beam. Load $q(z)$ acts on $z = 0 \sim L$ in the beam. The cantilever beam actuator is suspended on the fixed electrode, indicated in Figure 1. An electrostatic force, which is generated by the difference between

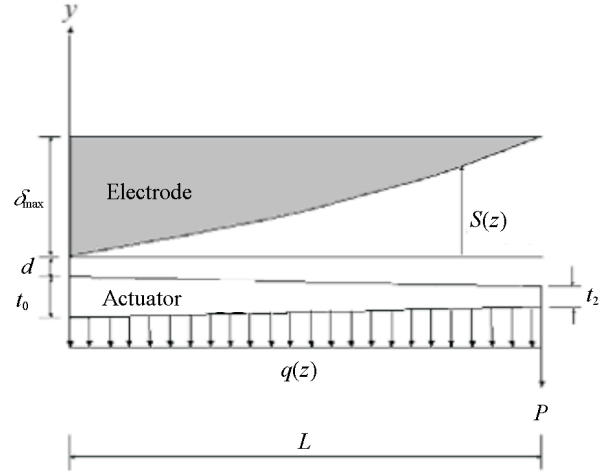


Figure 1. Schematic view of a curved electrode actuator.

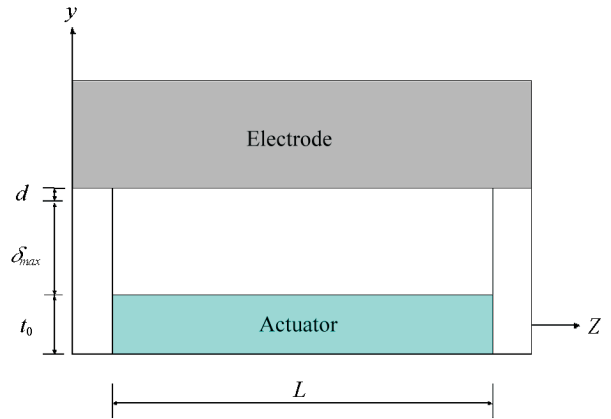


Figure 2. Schematic view of an electrostatic fixed-fixed actuator.

voltage applied to the curved electrode and that applied to the actuator, pulls the cantilever actuator toward to the curved electrode. Different electrode shapes have been presented to improve the distribution of electrostatic forces and the deformation of the actuator.

Figure 2 depicts a single type of actuator for a fixed-fixed beam suspended above a ground plane. When the external voltage e is applied between the deformable beam and the fixed electrode, a position-dependent electrostatic pressure is generated to pull the deformable beam toward to the ground electrode. This electrostatic pressure is approximately proportional to the inverse of the square of the gap between them. This approach depends on several approximations, including the parallel-plate approximation. When the voltage exceeds the critical voltage, the fixed-fixed beam is suddenly pulled into the electrode. The dielectric layer can

also prevent short-circuiting. The following analyses neglect the electric fringing effects.

The long beam assumption can be applied to simplify the strain energy of the bended actuator as

$$U = \frac{1}{2} \int_0^L EI \left(\frac{\partial^2 v(z)}{\partial z^2} \right)^2 dz \quad (9)$$

Considering the electrostatic force yields, the virtual work δW done by the bent actuator:

$$\delta W = \int_0^L \frac{\varepsilon_0 b e^2}{2 \left(d + S(z) + \frac{\beta z t_0}{2L} - v(z) \right)^2} \delta v dz - \int_0^L q(z) \delta v dz - P \delta v(L) \quad (10)$$

where E is Young's modulus of the actuator, e is the applied voltage, ε_0 is the dielectric constant of air ($\varepsilon_0 = 8.85 \times 10^{-12}$); b_0 is the width of the actuator, and d is the initial gap, as presented in Figure 1. The cross-sectional area of the tapered actuator is $A(z) = b_0 t_0 \left(1 + \beta \frac{z}{L} \right)$, where β is defined as the ratio $\frac{t_1 - t_0}{t_0}$. The moment of inertia of the cross-sectional area of the actuator is $I(z) = I_0 \left[1 + \beta \left(\frac{z}{L} \right) \right]^3$ with $I_0 = \frac{1}{12} b_0 t_0^3$. The shape function $S(z)$ describes the shape of the curved electrode, and is written as a polynomial, $S = \delta_{\max} \left(\frac{z}{L} \right)^n$. δ_{\max} is the gap between the tip of the curved electrode at $z = L$, and n is the polynomial order of the electrode shape. The shape of the electrode varies with n . Applying the principle of the total potential energy to Eqs. (9) and (10) yields,

$$\delta W - \delta U = 0 \quad (11)$$

The static deflection $v(z)$ of the actuator can be described by the following nonlinear equation:

$$\frac{d^2}{dz^2} \left(EI \frac{d^2 v(z)}{dz^2} \right) = \frac{\varepsilon_0 b e^2}{2 \left(d + S(z) + \frac{\beta z t_0}{2L} - v(z) \right)^2} - q(z) \quad (12)$$

The corresponding boundary conditions of the clamped-free actuator are,

$$v(0) = 0 \quad (13)$$

$$\frac{dv(0)}{dz} = 0 \quad (14)$$

$$EI \frac{d^2 v(L)}{dz^2} = 0 \quad (15)$$

$$\frac{d}{dz} \left[EI \frac{d^2 v(L)}{dz^2} \right] = P \quad (16)$$

The DQM is applied and Eq. (1) substituted into Eq. (12). Applying the boundary conditions allows the deflection equation of the actuator to be discretized the sample points as

$$[K]\{v\} = \{F\} \quad (17)$$

The Chebyshev-Gauss-Lobatto sampling point distribution yields the following elements in the stiffness matrices;

$$K_{11} = 1 \quad (18)$$

$$K_{1j} = 0 \quad \text{for } j = 2, 3, \dots, N \quad (19)$$

$$K_{2j} = \frac{D_{1j}^{(1)}}{L} \quad \text{for } j = 1, 2, \dots, N \quad (20)$$

$$K_{ij} = \frac{d^2}{dz^2} [EI(z)] \Big|_{z=z_i} \frac{D_{ij}^{(2)}}{L^2} + 2 \frac{d}{dz} [EI(z)] \Big|_{z=z_i} \frac{D_{ij}^{(3)}}{L^3} + EI(z_i) \frac{D_{ij}^{(4)}}{L^4} \quad (21)$$

for $i = 3, 4, \dots, N-2$ and $j = 1, 2, \dots, N$

$$K_{N-1,j} = EI(L) \frac{D_{N-1,j}^{(2)}}{L^2} \quad \text{for } j = 1, 2, \dots, N \quad (22)$$

$$K_{N,j} = \frac{d}{dz} EI(z) \Big|_{z=L} \frac{D_{N,j}^{(2)}}{L^2} + EI(L) \frac{D_{N,j}^{(3)}}{L^3} \quad (23)$$

for $j = 1, 2, \dots, N$

$$F_i = 0 \quad \text{for } i=1,2 \quad (24)$$

$$F_i = \frac{\varepsilon_0 b e^2}{2 \left(d + S + \frac{\beta z t_0}{2L} - v \right)^2} - q \quad (25)$$

$$\text{for } i = 3, 4, \dots, N-2$$

$$F_{N-1} = 0 \quad (26)$$

$$F_N = P \quad (27)$$

4. Numerical Results and Discussion

The tip deflections at various applied voltage for variously shaped electrodes are compared in Figure 3 to elucidate the feasibility of using DQM to solve the fixed-free beam type micro-actuator, and the accuracy of the method. Simulated results are compared with experimental data and the results in the literature [40]. The flat actuator is made of polysilicon. The material and the geometric

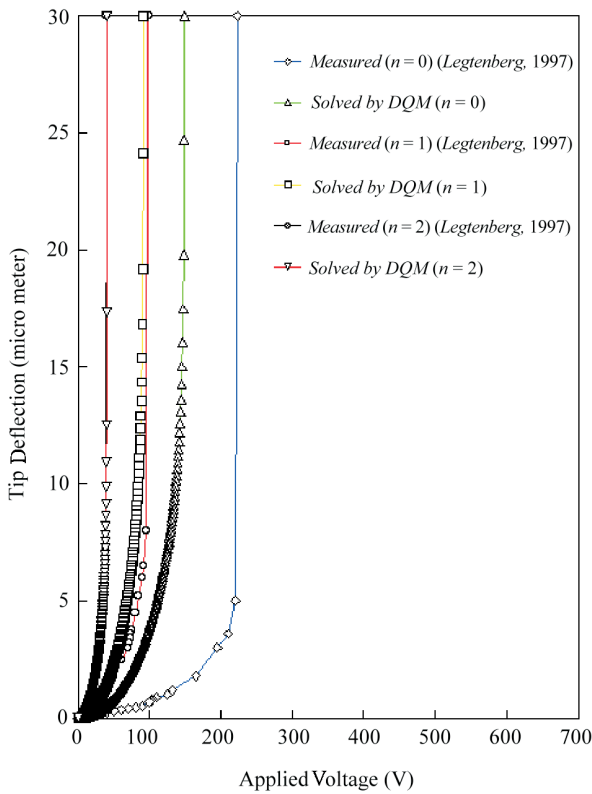


Figure 3. Comparison of the tip deflections with different applied voltages and electrode shapes.

parameters of the actuator are, [40] $E = 150.0 \text{ GPa}$, $\delta_{\max} = 30.0 \mu\text{m}$, $b_0 = 5.0 \mu\text{m}$, $t_0 = 2.0 \mu\text{m}$, $d = 2.0 \mu\text{m}$, $L = 500.0 \mu\text{m}$ and $\beta = 0.0$. The shape of the electrode varied with n , $n = 0, 1$ and 2 . The results imply that the static tip deflections calculated from the proposed DQM are very consistent with the experimental results published in the literature [40]. The effect of the shape of the electrode on the deflection of the tip in a curved electrode system was investigated using the DQM model proposed above.

The tip deflections of actuators corresponding to different values of β are compared in Figure 4. The material and the geometric parameters of the actuator are, $E = 150.0 \text{ GPa}$, $\delta_{\max} = 30.0 \mu\text{m}$, $b_0 = 5.0 \mu\text{m}$, $t_0 = 2.0 \mu\text{m}$, $d = 2.0 \mu\text{m}$, $L = 500.0 \mu\text{m}$ and $n = 2.0$. The effect of the actuator taper angle on the static deflection was examined. Numerical results reveal that the stiffness of the taper actuator is increased with the taper ratio β of the actuator. Results are calculated using the DQM model. The tip deflections with different applied voltages and value of $q(z)$ are compared in Figure 5. The pull-in voltage increases

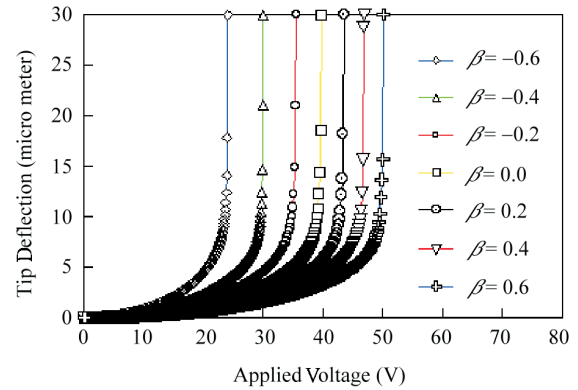


Figure 4. Comparison of the tip deflections with different values of β .

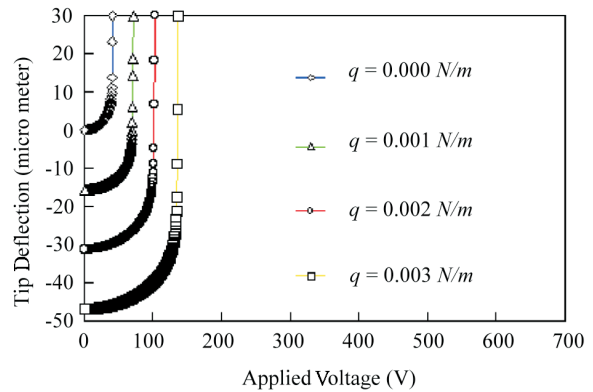


Figure 5. Comparison of the tip deflections with different applied voltages and loads q .

with the load $q(z)$. The accuracy of the calculated results implies that the static model derived from the DQM can be feasibly used to analyze the static deflection of the electrostatic actuator system. Figure 6 compares the tip deflections with different applied voltages and value of P . The pull-in voltage increases with the load P .

Figure 7 shows the variations in the deflection along the z direction in a fixed-fixed actuator with different applied voltage. The material and the geometric parameters of the actuator are, $E = 150.0 \text{ GPa}$, $\delta_{\max} = 30.0 \text{ }\mu\text{m}$, $b_0 = 5.0 \text{ }\mu\text{m}$, $t_0 = 2.0 \text{ }\mu\text{m}$, $d = 2.0 \text{ }\mu\text{m}$, $L = 500.0 \text{ }\mu\text{m}$ and $S = \delta_{\max}$. Numerical results imply that the DQM is a feasible and efficient method analyzing the nonlinear pull-in behavior of a fixed-fixed electrostatic micro-beam, which type is used extensively in micro-actuators and micro-sensors. Numerical results in this example demonstrate that the driving voltage significantly influences the

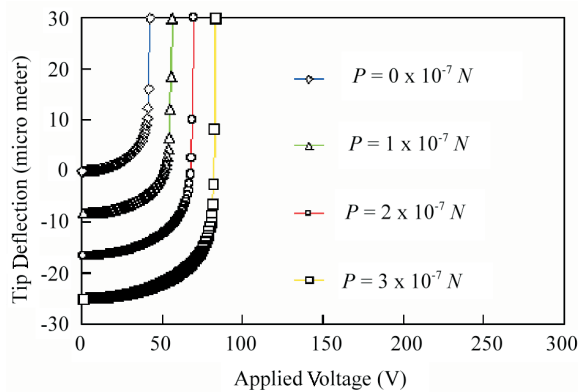


Figure 6. Comparison of the tip deflections with different applied voltages and loads P .

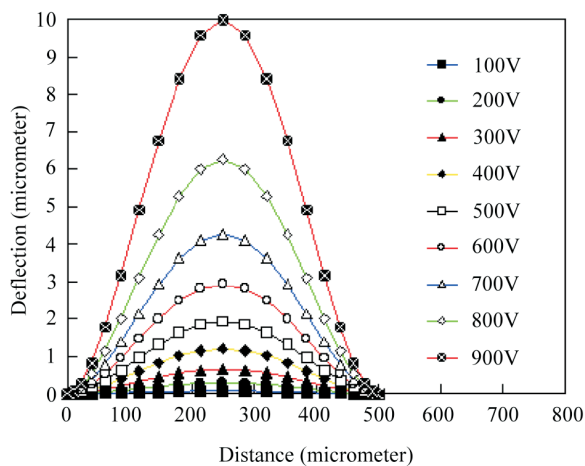


Figure 7. The variations in the deflection along the z direction in the fixed-fixed actuator with different applied voltages.

static behaviors of the actuator system.

5. Conclusions

DQM models for simulating the deflection and pull-in voltage of micro-actuators of the fixed-fixed and cantilever beam type are obtained. Numerical results imply that the DQM models can efficiently yield accurate results used to analyze the response of micro-actuator, which are used extensively in microelectromechanical systems. Numerical results indicate that DQM can efficiently provide accurate estimates of pull-in voltage for different types of electrostatic micro-actuators. The DQM is highly suited to designing or analyzing an electrostatic micro-actuator. More complicated models, such as those in which the shaped cantilever beam has variously curved electrodes, are also evaluated herein. The effects of the shape of electrode and the cantilever beam on the pull-in behavior of the tapered cantilever actuator in a micro-electrostatic-actuator system are investigated. The measured static deflections and the static deflections determined using the DQM are extremely consistent with the static deflections determined using the DQM. The simplicity of this formulation makes it a strong candidate for modeling more complicated applications.

References

- [1] Bellman, R. E. and Casti, J., "Differential Quadrature and Long-term Integration," *Journal of Mathematical Analysis and Application*, Vol. 34, pp. 235–238 (1971).
- [2] Bellman, R. E., Kashef, B. G. and Casti, J., "Differential Quadrature: A Technique for Rapid Solution of Nonlinear Partial Differential Equations," *Journal Computational Physics*, Vol. 10, pp. 40–52 (1972).
- [3] Bert, C. W., Jang, S. K. and Striz, A. G., "Two New Approximate Methods for Analyzing Free Vibration of Structural Components," *AIAA Journal*, Vol. 26, pp. 612–618 (1988).
- [4] Bert, C. W. and Mailk, M., "Differential Quadrature Method in Computational Mechanics: A Review," *Applied Mechanics Reviews*, Vol. 49, pp. 1–28 (1996).
- [5] Bert, C. W. and Malik, M., "Free Vibration Analysis of Tapered Rectangular Plates by Differential Quadrature Method: A Semi-analytical Approach," *Journal of Sound and Vibration*, Vol. 190, pp. 41–63 (1996).

- [6] Bert, C. W. and Malik, M., "On the Relative Effects of Transverse Shear Deformation and Rotary Inertia on the Free Vibration of Symmetric Cross-ply Laminated Plates," *Journal of Sound and Vibration*, Vol. 193, pp. 927–933 (1996).
- [7] Bert, C. W., Wang, X. and Striz, A. G., "Differential Quadrature for Static and Free Vibration Analysis of Anisotropic Plates," *International Journal of Solids and Structures*, Vol. 30, pp. 1737–1744 (1993).
- [8] Bert, C. W., Wang, X. and Striz, A. G., "Convergence of the DQ Method in the Analysis of Anisotropic Plates," *Journal of Sound and Vibration*, Vol. 170, pp. 140–144 (1994).
- [9] Jang, S. K., Bert, C. W. and Striz, A. G., "Application of Differential Quadrature to Static Analysis of Structural Components," *International Journal for Numerical Methods in Engineering*, Vol. 28, pp. 561–577 (1989).
- [10] Wang, X. and Bert, C. W., "A New Approach in Applying Differential Quadrature to Static and Free Vibrational Analyses of Beams and Plates," *Journal of Sound and Vibration*, Vol. 162, pp. 566–572 (1993).
- [11] Malik, M. and Bert, C. W., "Implementing Multiple Boundary Conditions in the DQ Solution of Higher-order PDE's Application to Free Vibration of Plates," *International Journal for Numerical Methods in Engineering*, Vol. 39, pp. 1237–1258 (1996).
- [12] Quan, J. R. and Chang, C. T., "New Insights in Solving Distributed System Equations by the Quadrature Method-I. Analysis," *Computers in Chemical Engineering*, Vol. 13, pp. 779–788 (1989).
- [13] Quan, J. R. and Chang, C. T., "New Insights in Solving Distributed System Equations by the Quadrature Method-II. Numerical Experiments," *Computers in Chemical Engineering*, Vol. 13, pp. 1017–1024 (1989).
- [14] Sherbourne, A. N. and Pandey, M. D., "Differential Quadrature Method in the Buckling Analysis of Beams and Composite Plates," *Computers and Structures*, Vol. 40, pp. 903–913 (1991).
- [15] Feng, Y. and Bert, C. W., "Application of the Quadrature Method to Flexural Vibration Analysis of a Geometrically Nonlinear Beam," *Nonlinear Dynamics*, Vol. 3, pp. 13–18 (1992).
- [16] Du, H., Lim, M. K. and Lin, R. M., "Application of Generalized Differential Quadrature Method to Structural Problems," *International Journal for Numerical Methods in Engineering*, Vol. 37, pp. 1881–1896 (1994).
- [17] Wang, X., Yang, J. and Xiao, J., "On Free Vibration Analysis of Circular Annular Plates with Non-uniform Thickness by the Differential Quadrature Method," *Journal of Sound and Vibration*, Vol. 184, pp. 547–551 (1995).
- [18] Liew, K. M., Han, J. B., Xiao, Z. M. and Du, H., "Differential Quadrature Method for Mindlin Plates on Winkler Foundations," *International Journal of Mechanical Sciences*, Vol. 38, pp. 405–421 (1996).
- [19] Liew, K. M., Han, J. B. and Xiao, Z. M., "Differential Quadrature Method for Thick Symmetric Cross-ply Laminates with First-order Shear Flexibility," *International Journal of Solids and Structures*, Vol. 33, pp. 2647–2658 (1996).
- [20] Du, H., Liew, K. M. and Lim, M. K., "Generalized Differential Quadrature Method for Buckling Analysis," *Journal of Engineering Mechanics*, Vol. 122, pp. 95–100 (1996).
- [21] Kang, K., Bert, C. W. and Striz, A. G., "Static Analysis of a Curved Shaft Subjected to End Torques," *International Journal of Solids and Structures*, Vol. 33, pp. 1587–1596 (1996).
- [22] Mirfakhraei, P. and Redekop, D., "Buckling of Circular Cylindrical Shells by the Differential Quadrature Method," *International Journal of Pressure and Piping*, Vol. 75, pp. 347–353 (1998).
- [23] Tomasiello, S., "Differential Quadrature Method: Application to Initial-boundary-value Problems," *Journal of Sound and Vibration*, Vol. 218, pp. 573–585 (1998).
- [24] Moradi, S. and Taheri, F., "Delamination Buckling Analysis of General Laminated Composite Beams by Differential Quadrature Method," *Composite: Part B*, Vol. 30, pp. 503–511 (1999).
- [25] Hsu, M. H., "Vibration Analysis of Edge-cracked Beam on Elastic Foundation with Axial Loading Using the Differential Quadrature Method," *Computer Methods in Applied Mechanics and Engineering*, Vol. 194, pp. 1–17 (2005).
- [26] Han, J. B. and Liew, K. M., "Axisymmetric Free Vibration of Thick Annular Plates," *International Journal of Mechanical Science*, Vol. 41, pp. 1089–1109 (1999).
- [27] De Rosa, M. A. and Franciosi, C., "Exact and Approx-

- mate Dynamic Analysis of Circular Arches Using DQM," *International Journal of Solids and Structures*, Vol. 37, pp. 1103–1117 (2000).
- [28] Sun, J. and Zhu, Z., "Upwind Local Differential Quadrature Method for Solving Incompressible Viscous Flow," *Computer Methods in Applied Mechanics and Engineering*, Vol. 188, pp.495–504 (2000).
- [29] Tanaka, M. and Chen, W., "Dual Reciprocity BEM Applied to Transient Elastodynamic Problems with Differential Quadrature Method in Time," *Computer Methods in Applied Mechanics and Engineering*, Vol. 190, pp. 2331–2347 (2001).
- [30] Striz, A. G., Chen, W. and Bert, C. W., "Static Analysis of Structures by the Quadrature Element Method (QEM)," *International Journal of Solids and Structures*, Vol. 31, pp. 2807–2818 (1994).
- [31] Wang, X. and Gu, H., "Static Analysis of Frame Structures by the Differential Quadrature Element Method," *International Journal for Numerical Methods in Engineering*, Vol. 40, pp. 759–772 (1997).
- [32] Gu, H. Z. and Wang, X. W., "On the Free Vibration Analysis of Circular Plates with Stepped Thickness Over a Concentric Region by the Differential Quadrature Element Method," *Journal of Sound and Vibration*, Vol. 202, pp. 452–459 (1997).
- [33] Chen, C. N., "The Warping Torsion Bar Model of the Differential Quadrature Element Method," *Computers & Structures*, Vol. 66, pp. 249–257 (1998)
- [34] Chen, W. L., Striz, A. G. and Bert, C. W., "High-accuracy Plane Stress and Plate Elements in the Quadrature Element Method," *International Journal of Solid and Structures*, Vol. 37, pp. 627–647 (2000).
- [35] Petersen, K. E., "Dynamic Micromechanics on Silicon: Techniques and Devices," *IEEE Transactions on Electron Devices*, Vol. ED-25, pp.1241–1250 (1978).
- [36] Osterberg, P. M., Yie, H., Cai, X., White, J. and Senturia, S., "Self-consistent Simulation and Modeling of Electrostatically Deformed Diaphragms," *Proceedings of IEEE Conference on Micro Electro Mechanical Systems*, pp. 28–32 (1994).
- [37] Gilbert, J. R., Legtenberg, R. and Senturia, S. D., "3D Coupled Electro-mechanics for MEMS: Application of CoSolve-EM," *Proceedings of IEEE Conference on Micro Electro Mechanical System*, pp. 122–127 (1995).
- [38] Elwenspoek, M., Weustink, M. and Legtenberg, R., "Static and Dynamic Properties of Active Joints," *The 8th International Conference on Solid-State Sensors and Actuators*, pp. 412–415 (1995).
- [39] Legtenberg, R., Berenschot, E., Elwenspoek, M. and Fluitman, J., "Electrostatic Curved Electrode Actuators," *Proceedings of IEEE Conference on Micro Electro Mechanical Systems*, pp. 37–42 (1995).
- [40] Legtenberg, R., Gilbert Senturia, J. S. D. and Elwenspoek, M., "Electrostatic Curved Electrode Actuators," *Journal of Microelectromechanical Systems*, Vol. 6, pp. 257–265 (1997).
- [41] Hirai, Y., Marushima, Y., Nishikawa, K. and Tanaka, Y., "Young's Modulus Evaluation of Si Thin Film Fabricated by Compatible Process with Si MEMS's," *International Conference on Microprocesses and Nanotechnology*, pp. 82–83 (2002).
- [42] Hirai, Y., Marushima, Y. and Soda, S., "Electrostatic Actuator with Novel Shaped Cantilever," *Proceedings of Internal Symposium on Micromechanics and Human Science*, pp. 223–227 (2000).
- [43] Hirai, Y., Shindo, M. and Tanaka, Y., "Study of Large Bending and Low Voltage Drive Electrostatic Actuator with Novel Shaped Cantilever and Electrode," *Proceedings of Internal Symposium on Micromechanics and Human Science*, pp. 161–164 (1998).
- [44] Wang, P. K. C., "Feedback Control of Vibrations in a Micromachined Cantilever Beam with Electrostatic Actuators," *Journal of Sound and Vibration*, Vol. 213, pp. 537–550 (1998).
- [45] Shi, F., Ramesh, P. and Mukherjee, S., "Simulation Methods for Micro-electro-mechanical Structures (MEMS) with Application to a Microtweezer," *Computers & Structures*, Vol. 56, pp. 769–783 (1995).
- [46] Osterberg, P. M. and Senturia, S. D., "M-Test: A Test Chip for MEMS Material Property Measurement Using Electrostatically Actuated Test Structures," *Journal of Microelectromechanical Systems*, Vol. 6, pp. 107–117 (1997).
- [47] Gretillat, M. A., Yang, Y. J., Hung, E. S., Rabinovich, V., Ananthasuresh, G. K., Rooij, N. F. and Senturia, S. D., "Nonlinear Electromechanical Behavior of an Electrostatic Microrelay," *Proceeding of the International Conference on Solid-State and Actuators*, pp. 1141–1144 (1997).
- [48] Hung, E. S. and Senturia, S. D., "Extending the Travel Range of Analog-tuned Electrostatic Actuators," *Journal of Microelectromechanical Systems*, Vol. 8, pp.

- 497–505 (1999).
- [49] Chan, E. K., Garikipati, K. and Dutton, R. W., “Characterization of Contact Electromechanics Through Capacitance-voltage Measurements and Simulations,” *Journal of Microelectromechanical Systems*, Vol. 8, pp. 208–217 (1999).
- [50] Li, G. and Aluru, N. R., “Linear, Nonlinear and Mixed-regime Analysis of Electrostatic MEMS,” *Sensors and Actuators*, Vol. A91, pp. 278–291 (2001).
- [51] Chyuan, S. W., Liao, Y. S. and Chen, J. T., “An Efficient Method for Solving Electrostatic Problems,” *Computing in Science & Engineering*, Vol. 5, pp. 52–58 (2003).
- [52] Chyuan, S. W., Liao, Y. S. and Chen, J. T., “Computational Study of Variations in Gap Size for the Electrostatic Levitating Force of MEMS Device Using Dual BEM,” *Microelectronics Journal*, Vol. 35, pp. 739–748 (2004).
- [53] Liao, Y. S., Chyuan, S. W. and Chen, J. T., “Efficaciously Modeling the Exterior Electrostatic Problems with Singularity for Electron Devices,” *Circuits and Devices Magazine*, Vol. 20, pp. 25–34 (2004).

Manuscript Received: Apr. 14, 2005

Accepted: Sep. 2, 2005